Proceedings of the ASME 2011 Dynamic Systems and Control Conference
DSCC2011
October 31 - November 2, 2011, Arlington, VA, USA

DSCC2011-6030

MODEL PREDICTIVE CONTROL OF A MICROGRID WITH PLUG-IN VEHICLES: ERROR MODELING AND THE ROLE OF PREDICTION HORIZON

Diane L. Peters*
Abigail R. Mechtenberg
John Whitefoot
Panos Y. Papalambros
Department of Mechanical Engineering
University of Michigan
Ann Arbor, Michigan 48109
Email: dlpeters@umich.edu, amechten@umich.edu, johnjohn@umich.edu, pyp@umich.edu

ABSTRACT

We demonstrate the use of model predictive control (MPC) for a microgrid with plug-in vehicles. A predictive model is developed based on a hub model of the microgrid, and the control is optimized for minimum generator fuel usage. A variety of horizons and levels of prediction error are used in the optimization. A new method to model expected load and error is presented based on radial basis functions. Results show that for a given prediction horizon, as the level of prediction error increases, the amount of fuel used increases. Results also show that in some cases there is little benefit in extending the prediction horizon. While an extended prediction horizon does result in increased use of battery storage, this does not necessarily produce significant decreases in fuel usage. This result is analyzed and explained in terms of battery charging and discharging limitations.

1 INTRODUCTION

Recently, the control of electrical microgrids has been the focus of research efforts. A microgrid typically covers a small geographic area and contains both loads and localized energy generation and storage resources. These microgrids have the ability to operate either in coordination with or isolated from an external electrical grid. They are particularly useful when energy security is important or where electrical distribution infrastructure does not exist. A few examples of such situations are military bases [1], medical complexes, island communities [2], and remote towns [3, 4].

Microgrid control may be addressed at two different time scales, a long time scale dispatch problem in which power from distributed energy sources is allocated to various loads and storage devices, and a regulation problem in which short time scales are considered and the key issues are system stability and power quality. In this work, we address the dispatch control problem. This dispatch problem is often solved in practice with a rule-based approach over a single time instance, such as that developed by HOMER Energy [5]. This approach solves the dispatch problem by minimizing a cost function over a single time increment without considering the benefits of storing energy for use in future time increments [6]. The rule-based approach used by HOMER was compared to a forward-looking dispatch strategy, in the context of sizing the system components, by Whitefoot et al. [7], and it was found that the forward-looking dispatch strategy offers some advantage over the rule-based approach, especially for energy storage management.

A variety of control techniques have been considered for microgrids, including centralized and decentralized controls on a number of different time scales, as described in [8]. One technique which has been applied to microgrids is predictive control, with the system design fixed. Arnold et al. applied predictive control to a system with combined electricity and natural

*Address all correspondence to this author.

gas [9]. The controller was implemented in a distributed fashion, in which control is spread over the individual hubs. In this implementation, the future was assumed to be perfectly forecasted. Closer to our present approach, del Real et al. [10] applied model predictive control (MPC) to a two-generator power plant with solar panels and a fuel cell. This work showed that MPC could be used to achieve effective reference tracking while operating in an efficient way. In that work, only a single day was considered for the control.

While MPC is a widely used technique for process control, it can be computationally demanding. A sufficiently long horizon must be chosen in order to provide a stable controller [11], as well as to insure that a feasible solution can be found [12]. The need for a long horizon will greatly increase the dimensionality of the problem. If the MPC problem is an unconstrained linear optimization, then it is simply a least-squares problem [11]; if the MPC problem is a constrained linear optimization, it can also be solved explicitly [12]. However, if the objective function is nonlinear, then the techniques developed to find an explicit solution are not applicable.

It is also important, when formulating an MPC problem, to consider the effect of prediction error. The first, and most widely used, method for handling prediction error is to minimize the cost function for the most expected situation [13]. Another method which has been used is to consider the worst situation [13], i.e., to formulate the optimization as a minimax problem [14]. This may be an overly conservative approach, particularly when the worst-case scenario has a low probability of occurrence, and can lead to a sub-optimal controller in the majority of cases which are likely to occur.

In this work, we consider the use of predictive control for a year, with a given (fixed) microgrid design. This design includes both dispatchable and non-dispatchable power sources, stationary battery storage, and the use of plug-in hybrid electric vehicles for auxiliary energy storage. While a microgrid has multiple layers of control, addressing both power flow (i.e., the scheduling problem) and power stability, in this work we are only addressing the scheduling problem. We consider a variety of different horizon lengths, under varying levels of prediction error. This prediction error is introduced into the power load profiles of the buildings and into the derating factor of the solar panels which supply power to the system. We show that, as prediction error increases, the amount of fuel required will increase for a given length of prediction horizon. We also show that a longer prediction horizon will result in increased use of battery storage. This increased use of battery storage does not necessarily reduce fuel use, however, and we discuss the reasons why this may be true.

The paper is organized as follows. In Section 2, we describe the specific case study used in this paper, and present a method for modeling the predicted load and prediction errors based on radial basis functions. In Section 3, we show how the model used by del Real et. al [6] can be used to model this system, then transform it into a discrete model in state-space form. In Section 4, we formulate the optimal control problem. In Section 5, we present results of the optimal control design for variations in prediction error and prediction horizon. Concluding remarks are given in Section 6.

2 MODELING OF CASE STUDY

In this study, we consider a simple microgrid, such as might be constructed at a military Forward Operating Base (FOB). This microgrid consists of buildings, a vehicle charging station, stationary battery storage, solar panels, and a diesel generator, as shown in Figure 1. Each of these components is described in more detail below, and relevant parameters are given in Table 1.

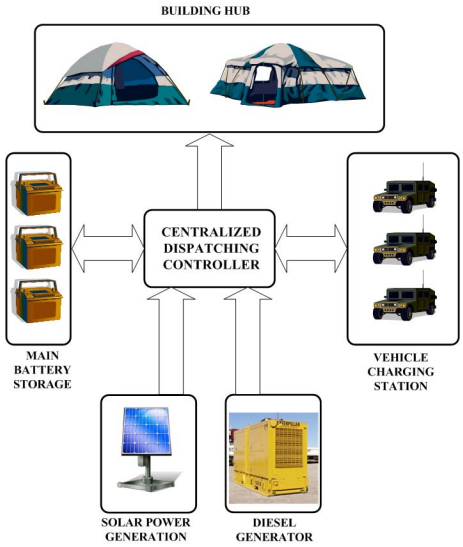

FIGURE 1. Schematic of Microgrid

TABLE 1. Parameters for Microgrid and Vehicles

Design	**Rated Power** or **Capacity** (total)
Main Generator	55 kW
Solar Panels	55 kW
Main Batteries	75 kWh
10 Vehicles	100 kWh
Power Load	50 kW

2.1 BUILDINGS

Three buildings are present in this microgrid. Since detailed field data is not available for the power usage at FOBs, a power load profile was postulated. The value of 2 kW/soldier was used to generate daily and seasonal power loads for an entire FOB, with the variations in power load based on engineering intuition. The load is modeled using a radial basis function, with the functional form shown below:

$$P(t) = P_{base} + P_{diurnal}(t, \sigma_H, \mu_H, \sigma_L, \mu_L) + P_{season}(t, T_H, T_L) \quad (1)$$

where P_{base} is the base power load in kW, $P_{diurnal}$ is the diurnal variations of the load which depends on the hour of the peak and trough load $\mu_{H,L}$ as well as the width of the peak and trough load $\sigma_{H,L}$, and P_{season} is the season variations of the load which depends on the high and low temperatures. Three of these values are known for a specific location of a forward operating base, P_{base}, T_{High}, and T_{Low}, with a known number of soldiers at that base. The other four values are estimated based on normal patterns of behavior, assuming that the peak load can be as high as 3 times the base load and trough load can be as low as 60% of the base load (although we add error to these values so that it can be greater or less than these initial intuition values). The following is the diurnal variability for one building:

$$P_{diurnal}(t) = \sum_{i=1}^{days} \left[\begin{array}{l} 3P_{base}\left(\frac{1}{\sqrt{2\pi\sigma_H^2}} e^{\frac{-(t-(\mu_H-(i-1)*24))^2}{2\sigma_H^2}}\right) \\ -0.6P_{base}\left(\frac{1}{\sqrt{2\pi\sigma_L^2}} e^{\frac{-(t-(\mu_L-(i-1)*24))^2}{2\sigma_L^2}}\right) \end{array} \right] \quad (2)$$

By using this formulation, we can add random noise to the hour of the peak or trough load independently from the width of the peak or trough load. We can also add random noise, again independently, to the base load. For example, the following equation shows five unique places where errors can be added to the forecasted power load, with the relationship between these errors and the nominal power load shown in Figure 2.

$$P_{\in}(t) = \sum_{i=1}^{days} \left[\begin{array}{l} 3P_{\in_1}\left(\frac{1}{\sqrt{2\pi\sigma_{H_{\in_2}}^2}} e^{\frac{-\left(t-\left(\mu_{H_{\in_3}}-(i-1)*24\right)\right)^2}{2\sigma_{H_{\in_2}}^2}}\right) \\ -0.6P_{\in_1}\left(\frac{1}{\sqrt{2\pi\sigma_{L_{\in_4}}^2}} e^{\frac{-\left(t-\left(\mu_{L_{\in_5}}-(i-1)*24\right)\right)^2}{2\sigma_{L_{\in_4}}^2}}\right) \end{array} \right] \quad (3)$$

where $\in_1$ is the error to the base power load, $\in_2$ and $\in_3$ are the errors to the peak time and width, and $\in_4$ and $\in_5$ are the errors to the trough time and width.

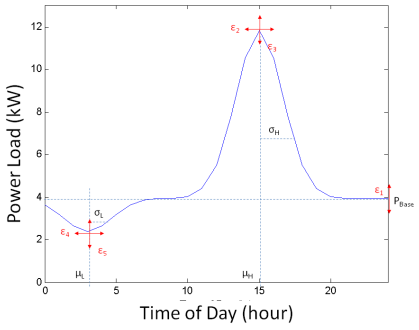

FIGURE 2. Diurnal Load for One Day without Random Noise

The following is the temperature variability based on high and low temperatures:

$$T_{season}(t) = T_{average} + (T_{High} - T_{average}) sin(t\pi/12) \quad (4)$$

This temperature seasonal modeling assumes that during the day, the temperature fluctuates as a sine function between the high and low temperatures. Based on monthly high and low temperatures, the power load varies seasonally because more HVAC is needed in extreme temperatures (either hot or cold). This additional variability was also described in [7], though it was modeled in a different fashion, and is shown in Figure 3.

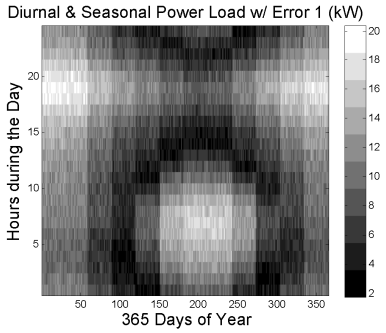

FIGURE 3. Density Map of Diurnal and Seasonal Load from One Building for One Year

2.2 HOMER ENERGY'S SOLAR AND BATTERY MODELS

HOMER Energy is a well-established software program for designing microgrids. Since its solar and battery models have been successfully used in a variety of microgrid applications, we chose to adopt those models for this work. The solar model was modified, however, in order to incorporate a random prediction error for this study.

The solar energy generation calculations in HOMER use the following model [5]:

$$P_{solarpanel} = f_{PV_{\in}} Y_{PV} \frac{I_T}{I_S} \tag{5}$$

where f_{PV} is the derating factor and where we add random noise, Y_{PV} is the rated capacity of the solar panel which we designed as 55 kW, I_T is the global solar radiation incident on the surface of the panel, and I_S is the 1 kW/m^2 [5]. In this study, we chose to incorporate the random term into the derating factor. This derating factor, which is "meant to account for effects of dust on the panel, wire losses, elevated temperature, or anything else that would cause the output of the PV panels to deviate from that expected under ideal conditions." [5] can be held constant in the HOMER Energy model or vary according to temperature linearly (although they describe it as varying the solar panel efficiency and not as varying the derating factor). We talk about this error, ε_6, as the derating factor to be consistent in the modeling and for future work to incorporate dust storms or snow for FOBs in the desert or mountains, respectively.

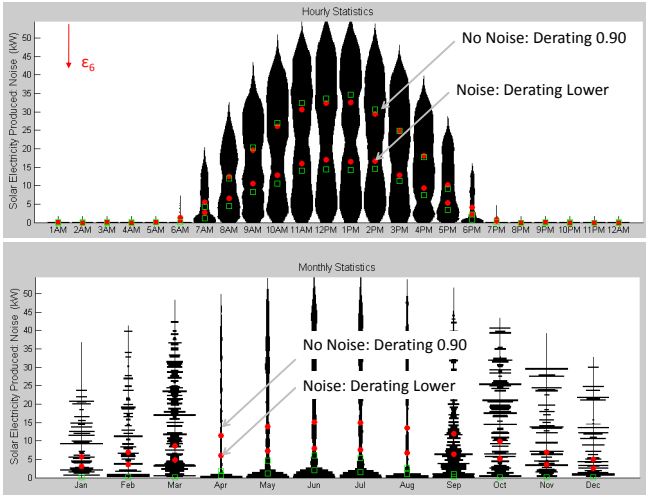

FIGURE 4. Hourly and Monthly Distribution Plots of Solar Power Generator without and with large Random Noise $\in_6$

Figure 4 illustrates a significant derating factor change from 0.90 to 0.50 and therefore would decrease the electricity produced from these solar panels significantly. In the hourly graph, midday generation drops from average of approximately 35 kW to 17 kW. In the monthly graph, the June average generation drops from 15 kW to 7.5 kW. Even though the statistics of the distribution plots vary, the pattern is the same.

In general, the change of temperatures of the batteries would dramatically change the performance of the batteries. In this study, it is assumed that the batteries will not experience significant changes in ambient temperature because they will be indoors or in an environmentally controlled enclosure, and therefore this temperature dependence is not included. Consequently, we modeled a lead-acid battery model, similar to what is found in the default list in HOMER. Parameters for the battery model are given in Table 2.

TABLE 2. Characteristics of Main Storage Battery

Characteristic	**Value**
Capacity	75 kWh
Round trip efficiency	81%
Minimum State of Charge (SOC)	20%
Maximum State of Charge (SOC)	80%
Maximum Charge Rate	7.5 kW
Maximum Discharge Rate	3.8 kW

2.3 MAIN GENERATOR

The main generator model calculates the generator fuel usage, in liters, based on the amount of power required from the generator. Using data from fifty Cummins diesel gensets, a surrogate model for efficiency, generator rated power, and percentage of load was created.

The surrogate model is given by Eq. (7), and it fits to the data with a calculated R^2 value of 0.94.

$$\eta = \begin{array}{c} 0.3461 + 0.0002P - 0.0561X_{\%load} \\ +0.0025log(P+0.01) + 0.0828log(X_{\%load}+0.01) \end{array} \tag{6}$$

$$L(L/hr) = \frac{P_{elec}(kW)}{\eta} = \frac{0.1011PX_{\%load}}{E} \tag{7}$$

where 0.1011 is the unit conversion between kW and L/hr for rate of energy conversion. For this case study, we choose a 55 kW diesel generator, and therefore the fuel usage is given by the equation:

$$L = \frac{5.5605 X_{\%load}}{0.3658 - 0.0561 X_{\%load} + 0.0828 log(X_{\%load} + 0.01)} \quad (8)$$

2.4 VEHICLE CHARGING STATION

Ten plug-in vehicles are intermittently connected to the microgrid. It is assumed that the scheduling of the vehicles is known *a priori*, and that this schedule is identical for every day of the time period considered. It is assumed that every vehicle returns to the charging station with its battery in the same state as when it left. Scheduling for the vehicles over the course of the day is given in Figure 5.

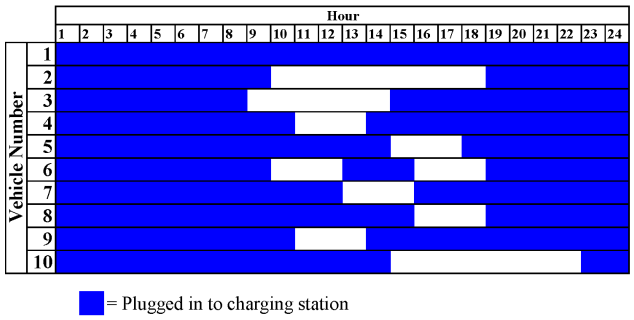

FIGURE 5. Daily Scheduling of Plug-In HEVs

The vehicle batteries are assumed to be nickel-metal hydride batteries, and are all identical in their upper and lower charge limits and their charging and discharging rates, as given in Table 3. When a vehicle is not connected to the microgrid, it is not possible to charge or discharge its battery. The effective charge level and total storage capacity of the vehicles, therefore, will change in a discontinuous fashion as vehicles are connected and disconnected. The central controller for the microgrid treats the vehicle charging station as a single unit, sending it a single power flow which is then split among the vehicles. The vehicle charging station uses a rule-based approach to allocate power, setting a priority on each vehicle according to its current SOC.

3 SYSTEM MODELING

The general system description for a microgrid may be initially formulated in the form used by del Real et al. [6]:

$$\boldsymbol{L} = \boldsymbol{C}\boldsymbol{P} - \boldsymbol{S}\dot{\boldsymbol{E}} \quad (9)$$

TABLE 3. Characteristics of Vehicle Batteries

Characteristic	Value
Capacity	10 kWh
Round trip efficiency	81%
Minimum State of Charge (SOC)	40%
Maximum State of Charge (SOC)	60%
Maximum Charge Rate	1.0 kW
Maximum Discharge Rate	0.5 kW

where $\boldsymbol{L}$ is the vector of power loads at each hub, $\boldsymbol{C}$ is the converter coupling matrix, $\boldsymbol{P}$ is the vector of power generated by each power source, $\boldsymbol{S}$ is the storage coupling matrix, and $\dot{\boldsymbol{E}}$ is the rate of change of the charge in each storage device. In our system formulation, this set of equations is then reduced to eliminate those that do not contain a dispatchable power source or dispatchable energy storage. The resulting system of equations is then partitioned as follows:

$$\boldsymbol{L} = \begin{bmatrix} \boldsymbol{C}_{11} & \boldsymbol{C}_{12} \\ \boldsymbol{0} & \boldsymbol{C}_{22} \end{bmatrix} \begin{bmatrix} \boldsymbol{P}_{disp.} \\ \boldsymbol{P}_{non-disp.} \end{bmatrix} - \begin{bmatrix} \boldsymbol{0} & \boldsymbol{0} \\ \boldsymbol{S}_{21} & \boldsymbol{S}_{22} \end{bmatrix} \begin{bmatrix} \boldsymbol{0} \\ \dot{\boldsymbol{E}} \end{bmatrix} \quad (10)$$

where $\boldsymbol{P}_{disp}$ is the vector of dispatchable (controllable) power sources, and $\boldsymbol{P}_{non-disp}$ is the vector of non-dispatchable power sources, such as wind and solar power. This can then be transformed into the form

$$\begin{bmatrix} \dot{\boldsymbol{E}} \\ \boldsymbol{P}_{disp} \end{bmatrix} = \begin{bmatrix} \boldsymbol{S}_{22}^{-1} \\ \boldsymbol{C}_{11}^{-1} \end{bmatrix} \boldsymbol{L} - \begin{bmatrix} \boldsymbol{S}_{22}^{-1}\boldsymbol{C}_{22} \\ \boldsymbol{C}_{11}^{-1}\boldsymbol{C}_{12} \end{bmatrix} \boldsymbol{P}_{non-disp} \quad (11)$$

Since the matrices $\boldsymbol{C}$ and $\boldsymbol{S}$ are defined in terms of the dispatch factors used to control system power flow [6], this equation can then be written in state-space form, where the system states are the energy content of storage devices and the energy provided by dispatchable power sources. The problem may then be discretized and written in the form of a difference equation.

There will be one independent system state associated with each controllable power storage device, and one independent system state associated with each controllable power source. In our case study, the system is modeled as having four independent states: the total energy stored in the vehicle batteries, the energy stored in the main battery, the energy that has been output by the generator, and the excess energy that has been sent to ground. This excess energy state is included to provide for a situation where the solar power generated exceeds the building loads, and

the batteries are unable to store the excess. The system can then be described in the following form:

$$\begin{bmatrix} \dot{E}_v \\ \dot{E}_{mb} \\ \dot{E}_{excess} \\ P_{gen} \end{bmatrix} = L_B \begin{bmatrix} 1\,0\,0 \\ 0\,1\,0 \\ 0\,0\,1 \\ 1\,1\,1 \end{bmatrix} \boldsymbol{U} + \begin{bmatrix} -L_v \\ -L_{mb} \\ 0 \\ L_B - P_{solar} \end{bmatrix} \tag{12}$$

where the vector $\boldsymbol{U} = \frac{1}{u_B}[u_v\ u_{mb}\ u_{excess}]^T$. Each of the terms u_v, u_{mb}, and u_{excess} corresponds to the proportion of the available power from the generator and solar panel that is sent into the vehicle charging station, main storage battery, and sent to ground, respectively. The term u_B is the proportion of the available power used to supply the load. It is assumed that the full load demanded is supplied at all times, i.e., capacity shortages are not permitted. The subscripts *v*, *mb*, *excess*, *gen*, and *B* refer to the vehicles, main battery, excess power, generator, and buildings, respectively.

The power loss associated with the charging and discharging of the batteries is assumed to be proportional to the rate at which the batteries are charged or discharged. The power loss for the batteries can then be represented as

$$L_v = \mu_v \left|\dot{E}_v\right| \tag{13}$$
$$L_{mb} = \mu_{mb} \left|\dot{E}_{mb}\right| \tag{14}$$

where μ_v and μ_{mb} are assumed to be constant. The arithmetic sign of $\dot{E}$ is the same as the arithmetic sign of the corresponding dispatch factor U, and therefore the power losses can be described as

$$L_v = \mu_v \text{sign}\left(U_v\right) \dot{E}_v \tag{15}$$
$$L_{mb} = \mu_{mb} \text{sign}\left(U_{mb}\right) \dot{E}_{mb} \tag{16}$$

The system equation can then be re-written as

$$\begin{bmatrix} \dot{E}_v \\ \dot{E}_{mb} \\ \dot{E}_{excess} \\ P_{gen} \end{bmatrix} = L_B \begin{bmatrix} \frac{1}{1+\mu_v \text{sign}(U_v)} & 0 & 0 \\ 0 & \frac{1}{1+\mu_{mb}\text{sign}(U_{mb})} & 0 \\ 0 & 0 & 1 \\ 1 & 1 & 1 \end{bmatrix} \boldsymbol{U} + \begin{bmatrix} 0 \\ 0 \\ 0 \\ L_B - P_{solar} \end{bmatrix} \tag{17}$$

which is then discretized as

$$\begin{bmatrix} E_{v_{k+1}} \\ E_{mb_{k+1}} \\ E_{excess_{k+1}} \\ \sum_{i=1}^{k+1} P_{gen_i} \end{bmatrix} = T_s L_{B_k} \begin{bmatrix} \frac{1}{1+\mu_v \text{sign}\left(U_{v_k}\right)} & 0 & 0 \\ 0 & \frac{1}{1+\mu_{mb}\text{sign}\left(U_{mb_k}\right)} & 0 \\ 0 & 0 & 1 \\ 1 & 1 & 1 \end{bmatrix} \boldsymbol{U}_k + T_s \begin{bmatrix} 0 \\ 0 \\ 0 \\ L_{B_k} - P_{solar_k} \end{bmatrix} + \begin{bmatrix} E_{v_k} \\ E_{mb_k} \\ E_{excess_k} \\ \sum_{i=1}^{k} P_{gen_i} \end{bmatrix} \tag{18}$$

where T_s is the sampling time for the system control.

4 OPTIMAL CONTROL PROBLEM FORMULATION

In general, the objective function J in Model Predictive Control (MPC) is a penalty function that includes one term to penalize deviations from the desired trajectory and one term to penalize control effort [15]. In this problem, we choose the system trajectory to be of infinitely more importance than the effort required to accomplish this. The ability to meet the system's required power load is enforced through system constraints, and the penalty function is selected as the fuel required to run the diesel generator over the control horizon. The constraints are formulated to ensure that, at every time step, the SOC remains within given ranges for each battery, the charging or discharging rate of all batteries is within specified limits, and the generator is neither idling nor running beyond its maximum capacity. The optimization problem can then be expressed as

$$\min_{\boldsymbol{U}} J = \sum_{j=1}^{H} F\left(P_{gen_j}\right) \tag{19}$$

subject to

$$SOC_{v_{min}} \leq E_v \leq SOC_{v_{max}} \tag{20}$$
$$SOC_{mb_{min}} \leq E_{mb} \leq SOC_{mb_{max}} \tag{21}$$
$$MaxDischargeRate_v \leq \dot{E}_v \leq MaxChargeRate_v \tag{22}$$
$$MaxDischargeRate_{mb} \leq \dot{E}_{mb} \leq MaxChargeRate_{mb} \tag{23}$$
$$0.05 GeneratorSize \leq P_{gen} \leq GeneratorSize \tag{24}$$
$$0 \leq \dot{E}_{excess} \tag{25}$$

where H is the prediction horizon, $F\left(P_{gen_j}\right)$ is the fuel used to produce the generator power output, and the constraints must

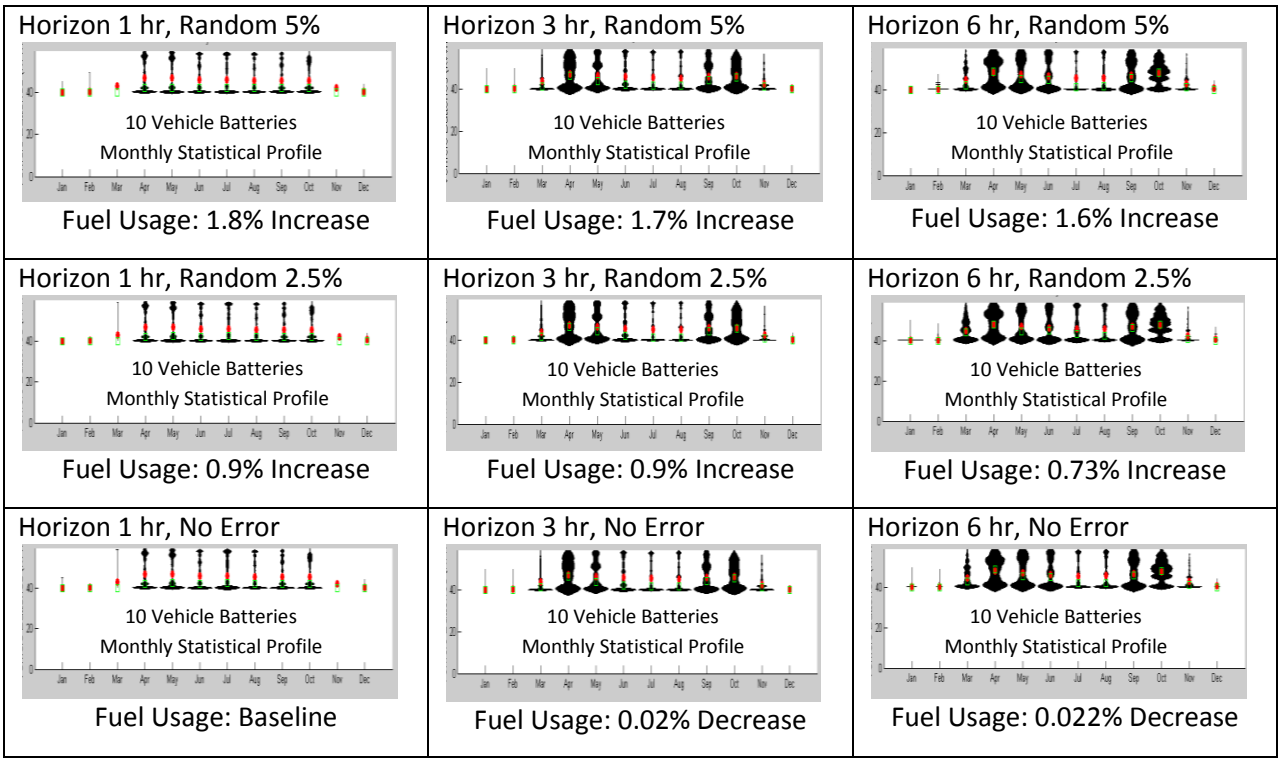

FIGURE 6. Profile of Vehicle Battery Charging as a Function of Time (January to December) including details of increase or decrease of fuel usage.

be met at every time step along that horizon. The fuel usage is calculated as described in Section 2.3. Since this function is non-linear, the techniques developed to solve linear MPC problems are not applicable, and the MPC problem was formulated as a non-linear constrained optimization problem and solved using Matlab's *fmincon* function at each time step. The time step for sampling and control implementation was selected to be one hour. A series of different horizons was used, with varying levels of random variability, and the results were compared.

5 RESULTS

Comparing the optimal results for differing levels of random prediction error and constant prediction horizon shows that fuel usage increases as the level of random error increases. These results are shown in Table 4 for a horizon of three hours, with the same pattern holding for other horizon lengths. While intuitive, this result underscores the need for an effective and efficient means of modeling such errors, such as the method presented here using radial basis functions. Such a method allows for the investigation of such effects.

Simulations of different prediction horizons and levels of random prediction error demonstrate that increasing the prediction horizon will change the SOC profile of the batteries as a function of time, as shown in Figure 6.

TABLE 4. Comparison of Random Error in Load and Solar Derating to Fuel Consumption (Horizon: 3 Hours)

Random Error	Fuel Consumption	Percent Increase
No Error	47.3 kL	–
2.5%	47.7 kL	0.85%
5.0%	48.4 kL	2.3%
10%	48.9 kL	3.4%

Although the batteries are used more for longer horizons, fuel consumption does not measurably decrease. This result can be explained by examining constraint activity. In those time steps where the power load for the buildings is significantly greater than the available solar power, constraints on the battery discharge rates for both the main battery and vehicle batteries are active. Similarly, when the amount of solar power available is significantly higher than the power load required by the buildings, constraints on the charging rates of both types of batteries are active. In this situation, excess power is produced which is

unable to be stored or used, and is thus wasted. This constraint activity, and the presence of excess power that cannot be stored for later use, suggests that battery charging and discharging rates will place more severe limitations than battery size on the performance of the microgrid.

6 CONCLUDING REMARKS

We proposed a methodology for using radial basis functions to model varying power loads with random errors of various magnitudes. This methodology was implemented in a case study, where model predictive control was used to solve the power dispatching problem for a simple microgrid using various prediction horizons. It was shown that a longer horizon does lead to increased battery usage, but does not necessarily result in a measurable decrease in fuel consumption. Constraint activity suggests that this is due to the limitations of the battery. This indicates that design of microgrids would benefit from insights into the limitations of batteries and the ability to effectively control them in such a system.

While the system considered in this work was a totally autonomous, or 'islanded', microgrid, a similar problem could be formulated for a grid-connected microgrid by choosing an objective function such as minimizing the power draw from that grid, minimizing the cost of electrical power, or some other appropriate metric. This problem may be a subject of future work. Future work in this area may also include the use of higher fidelity component models, particularly for batteries. Investigation of the effects of various types and levels of prediction errors is also a promising area. The interaction between the vehicle charging station and the centralized dispatching controller should also be investigated and tradeoffs between wind energy and solar energy explored. Power and energy tradeoffs are also an interesting area for future exploration, both in the area of microsources and in storage capability.

ACKNOWLEDGMENT

This work was supported by the Automotive Research Center, a US Army Center of Excellence in Modeling and Simulation of Ground Vehicles, headquartered at the University of Michigan. This support is gratefully acknowledged.

REFERENCES

[1] Shaffer, E. C., Massie, D. D., and Cross, J. B., 2006. Power and energy architecture for army advanced energy initiative. Tech. rep., Army Research Laboratory, Adelphi, MD.

[2] Tselepis, S., 2010. "Greek experience with microgrids: Results from the Gaidouromantra site, Kythnos island". In Vancouver 2010 Symposium on Microgrids.

[3] Ashok, S., 2007. "Optimised model of a community hybrid energy system". *Journal of Renewable Energy,* ***32***(7), p. 1155.

[4] Gupta, A., Saini, R. P., and Sharma, M. P., 2010. "Steady-state modelling of hybrid energy systems for off grid electrification of cluster of villages". *Journal of Renewable Energy,* ***35***(2), p. 520.

[5] Lambert, T., Gilman, P., and Lilienthal, P., 2006. "Micropower system modeling with Homer". In *Integration of Alternative Sources of Energy*, F. A. Farret and M. G. Simoes, eds. John Wiley & Sons, Inc., New York, NY, ch. 15.

[6] del Real, A. J., Galus, M. D., Bordons, C., and Andersson, G., 2009. "Optimal power dispatch of energy networks including external power exchange". In European Control Conference.

[7] Whitefoot, J. W., Mechtenberg, A. R., Peters, D. L., and Papalambros, P. Y., 2011. "Optimal component sizing and forward-looking dispatch of an electrical microgrid for energy storage planning". In Proceedings of the ASME 2011 International Design Engineering Technical Conferences & Computers and Information in Engineering Conference. Paper number DETC2011-48513 (accepted).

[8] Zamora, R., and Srivastava, A., 2010. "Controls for microgrids with storage: Review, challenges, and research needs". *Renewable and Sustainable Energy Reviews,* ***14***(7), pp. 2009–2018.

[9] Arnold, M., Negenborn, R. R., Andersson, G., and Schutter, B. D., 2009. "Multi-area predictive control for combined electricity and natural gas systems". In European Control Conference.

[10] del Real, A. J., Arce, A., and Bordons, C., 2007. "Hybrid model predictive control of a two-generator power plant integrating photovoltaic panels and a fuel cell". In Proceedings of the 46th IEEE Conference on Decision and Control.

[11] Garcia, C. E., Prett, D. M., and Morari, M., 1989. "Model predictive control: Theory and practice - a survey". *Automatica,* ***25***(3), p. 335.

[12] Bemporad, A., Borrelli, F., and Morari, M., 2001. "Model predictive control based on linear programming - the explicit solution". *IEEE Transactions on Automatic Control,* ***47***(12), p. 1974.

[13] Camacho, E. F., and Berenguel, M., 1997. "Robust adaptive model predictive control of a solar plant with bounded uncertainties". *International Journal of Adaptive Control and Signal Processing,* ***11***, p. 311.

[14] Scokaert, P. O. M., and Mayne, D. Q., 1998. "Min-max feedback model predictive control for constrained linear systems". *IEEE Transactions on Automatic Control,* ***43***(8), p. 1136.

[15] Camacho, E. F., and Bordons, C., 1999. *Model Predictive Control*. Springer-Verlag, New York, NY.